Progress In Electromagnetics Research C, Vol. 18, 31–45, 2011

HALF U-SLOT LOADED SEMICIRCULAR DISK PATCH ANTENNA FOR GSM MOBILE PHONE AND OPTICAL COMMUNICATIONS

J. A. Ansari and A. Mishra

Department of Electronics & Communication
University of Allahabad, Allahabad, India

B. R. Vishvakarma

Department of Electronics Engineering
I. T. BHU, Varanasi 221005, India

Abstract—In the present paper, a dual frequency resonance antenna is achieved by introducing half U-shaped slot in semicircular disk. It is analysed by using circuit theory concept. The resonance frequency is found to be 1.50 GHz and 2.32 GHz, and the bandwidth of the proposed antenna for lower and upper resonance frequency is found to be 5.96% and 11.08% respectively. It is found that the resonance frequency depends inversely on the slot length and feed point, while it increases with increasing the slot width and coaxial probe feed radius. The frequency ratio is found to be 1.54. The theoretical results are compared with IE3D simulation as well as reported experimental results, and they are in good agreement.

1. INTRODUCTION

The increasing use of wireless communication system demands antennas for different systems and standards with properties like compact, broadband and multiple resonant frequencies. In wireless communications, different systems and standard frequency bands are located, two of which are Global positing system (GPS) and Bluetooth. When a microstrip patch antenna is loaded with reactive elements such as slots [1–3], stubs or shorting pin [4–6], it gives tunable or dual frequency antenna characteristics.

Received 7 October 2010, Accepted 15 November 2010, Scheduled 22 November 2010
Corresponding author: Jamshed Aslam Ansari (jaansari@rediffmail.com).

A slot antenna has special advantage because of its simple structure, such as wider bandwidth, less conductor loss [7–11]. A probe feed microstrip antenna with an internal U-shaped slot having large impedance bandwidth with broad side radiation pattern is reported [12, 13].

Here we have proposed new patch antenna configuration that can have dualband operation. The proposed antenna is semicircular half U-slot loaded patch that provides a significant size reduction and large impedance bandwidth with broad side radiation pattern. Dual frequency is tuned by changing the dimensions of the slot. A parametric study has been carried out using the circuit theory concept by varying the length, width of the slot, feed location and probe radius. Various antenna parameters are calculated as a function of frequency for different value of slot length, width, feed point and probe radius.

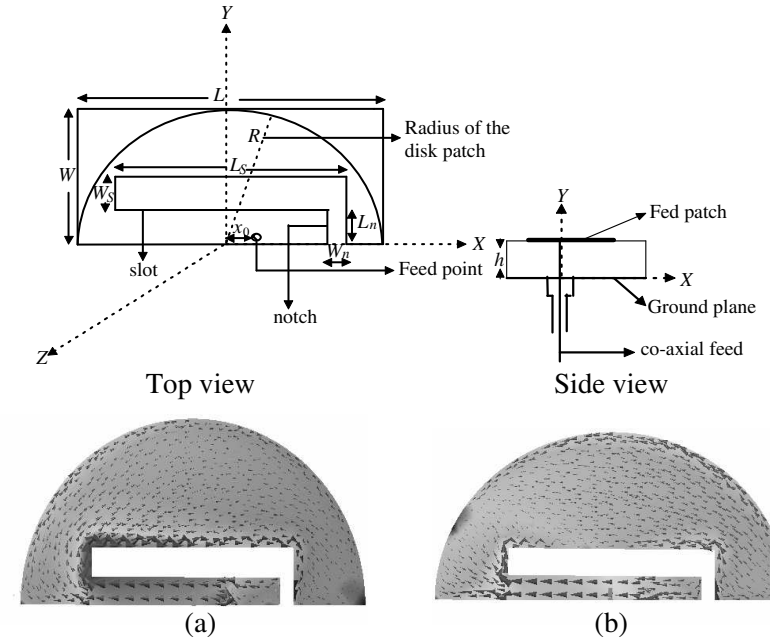

Figure 1. Antenna geometry and its current distribution for lower and upper resonance frequency. (a) $fr_1 = 1.49\,\text{GHz}$. (b) $fr_2 = 2.29\,\text{GHz}$.

2. CONFIGURATION AND ANALYSIS

Figure 1 shows the side and top view geometries for the proposed antenna with current distribution. Analysis of the half disk patch antenna is similar to that of circular disk patch, but the effective radius changes due to 50% reduction in size. The resonance frequency of half circular disk patch is given as [14]

$$f_r = \frac{k_{nm}c}{2\pi a_e\sqrt{\varepsilon_e}} \tag{1}$$

where k_{nm} is the mth zero root of the derivative of Bessel function of order n; c is the velocity of light; and ε_e is the effective dielectric constant of the substrate [15]. a_e effective radius of the half disk patch is given as

$$a_e = \sqrt{\frac{L_eW_e}{\pi}}.$$

A half circular disk patch is analyzed by supposing it equivalent to a rectangular patch with dimensions $L \times W$ [16], where $L = 2a$ and $W = \frac{\pi a}{4}$. The effective radius a_e of the half disk is calculated by equating the area of half disk to the expanded rectangular patch with dimension $(L_e \times W_e)$, where L_e and W_e are effective length and width of the rectangular patch and can be calculated by [16]. The equivalent circuit of the half circular disk patch is shown in Fig. 2 in which the circuit parameters, i.e., resistance (R_1) inductance (L_1), and capacitance (C_1) are calculated by [15].

$$C_1 = \frac{\varepsilon_e\varepsilon_0 LW}{2h}\cos^{-2}(\pi x_0/L) \tag{2}$$

$$L_1 = \frac{1}{\omega^2 C_1} \tag{3}$$

$$R_1 = \frac{Q_r}{\omega C_1} \tag{4}$$

in which

L = length of the rectangular patch
W = width of the rectangular patch
x_0 = feed point location along length of the patch
h = thickness of the substrate material

and

$$Q_r = \frac{c\sqrt{\varepsilon_e}}{fh}$$

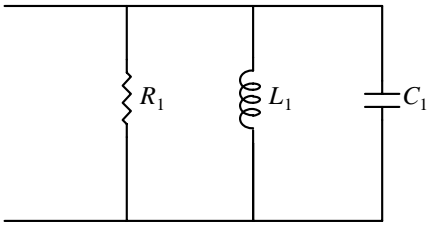

Figure 2. Equivalent circuit of semicircular disk patch.

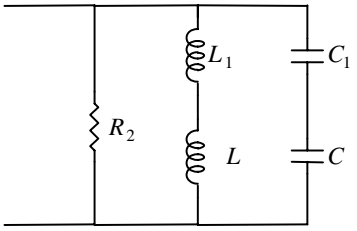

Figure 3. Equivalent circuit of semicircular disk patch due to effect of notch.

where

c = velocity of light

f = design frequency

ε_e = effective permittivity of the medium which is given by [16]

$$\varepsilon_e = \frac{\varepsilon_e + 1}{2} + \frac{\varepsilon_e - 1}{2}\left(1 + \frac{10h}{W}\right)^{-1/2}$$

where, ε_e = relative permittivity of the substrate material. The analysis of the proposed antenna is classified in two parts.

2.1. Analysis of Slot Loaded Semicircular Disk Patch Antenna

When the slot is embedded in the patch, having dimension $(L_S \times W_S)$, it can be analysed by using the duality relationship between the dipole and slot [17]. The radiation resistance of slot on the half disk patch can be given as

$$R_r = \frac{\eta_0 \cos^2 \alpha}{2\pi} \int_0^{\pi} \left[\frac{\left[\cos \frac{k^2 \cos\theta}{2} - \cos \frac{kL_S}{2}\right]^2}{\sin\theta} \right] d\theta \tag{5}$$

which yields

$$R_r = 60C + \ln(kL_S)C_i(kL_S) + \frac{1}{2}\sin(kL_S)[S_i(2kL_S)2S_i(kL_S)]$$
$$+\frac{1}{2}\cos(kL_S)C + \ln\frac{kL_S}{2} + C_i(2kL_S)2C_i(kL_S)$$

in which C is Euler's constant = 0.5772 and S_i and C_i are the sine and cosine integrals defined as

$$S_i(x) = \int_0^x \frac{\sin(x)}{x} dx$$

and

$$C_i(x) = -\int_0^\infty \frac{\sin(x)}{x} dx$$

Now the total input impedance of the slot can be given as [18].

$$Z_{\text{slot}} = \frac{\eta_0^2}{4Z_{cy}} \tag{6}$$

in which

$$\eta_0 = 120\pi$$

and

$$Z_{cy} = R_r(kL_S) - j\left[120\left(\ln\left(\frac{L_S}{W_S}\right) - 1\right)\cot\left(\frac{kL_S}{2}\right) - X_r\left(kL_S\right)\right]$$

where, R_r is the real part and equivalent to the radiation resistance of slot and X_r is the input reactance of the slot and given as [17].

$$X_r = 30\cos^2\alpha\Big\{2S_i(kLs) + \cos(kLs)[2S_i(kLs) - S_i(2kLs) - \sin(kLs)]$$
$$\left[2C_i(kLs) - C_i(2kLs) - C_i\left(\frac{2kWs^2}{Ls}\right)\right]\Big\}$$

in which L_S, W_S are length and width of the slot.

2.2. Analysis of Notch Loaded Semicircular Patch Antenna

When the notch is incorporated in the half disk patch ($L_n \times W_n$), two currents flow in the patch, and one is the normal patch current and resonates at the design frequency of the initial patch. However, the other current flows around the notch resulting in the second resonance frequency. Discontinuities due to notch incorporated in the patch are considered in terms of an additional series inductance (ΔL) and series capacitance (ΔC) that modify the equivalent circuit of RMSA as shown in Fig. 3, in which series inductance (ΔL) and series capacitance (ΔC) can be calculated as [19, 20].

$$\Delta L = \frac{h\mu_0\pi}{8}(L_n/L)^2$$

and

$$\Delta C = \left(\frac{L_n}{L}\right) \cdot C_g$$

where

μ_0 = $4\pi \times 10^{-7}$ H/m
L_n = depth of the notch
C_g = gap capacitance and is given by [21].

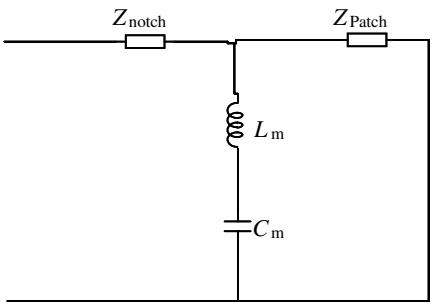

Figure 4. Equivalent circuit of coupled notch loaded semicircular disk patch antenna.

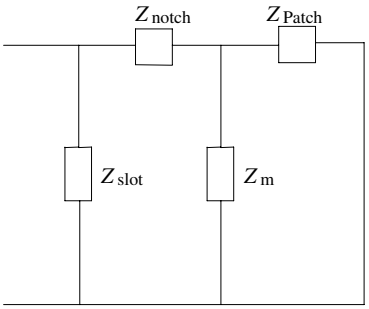

Figure 5. Equivalent circuit of half U-slot loaded semicircular disk patch antenna.

The value of resistance R_2 after cutting the notch is calculated by [22]. It may be noted that the two resonant circuits, one of which is the initial RLC of the half disk patch and shown in Fig. 2 and the other one is after cutting the notch (Fig. 3), are coupled through mutual inductance (L_m) and mutual capacitance (C_m). Thus the equivalent circuit of the notch loaded patch antenna can be given as shown in Fig. 4.

Hence the total input impedance of proposed antenna can be calculated from Fig. 5 as

$$Z_{Total} = (Z^*) + \frac{Z_m Z_{patch}}{Z_{patch} + Z_m} \tag{7}$$

where

$$Z^* = \frac{Z_{slot} Z_{notch}}{Z_{slot} + Z_{notch}} \tag{8}$$

where Z_{patch} is the input impedance of the microstrip patch antenna can be calculated from Fig. 2 as

$$Z_{Patch} = \frac{1}{\frac{1}{R_1} + j\omega C_1 + \frac{1}{j\omega L_1}}$$

and

$$Z_{notch} = \frac{j\omega R_1 L_2}{j\omega L_2 + R_1 - R_1 L_2 C_2 \omega^2}$$

in which

$$\begin{aligned} L_2 &= L_1 + \Delta L \\ C_2 &= \frac{C_1 \Delta C}{C_1 + \Delta C} \end{aligned}$$

and

$$Z_m = \left(j\omega L_m + \frac{1}{j\omega C_m} \right)$$

where L_m and C_m are the mutual inductance and mutual capacitance between two resonant circuits and given as [21].

$$L_m = \frac{C_p^2(L_1 + L_2) + \sqrt{C_p^2(L_1 + L_2)^2 + 4C_p^2(1 - C_p^2)L_1L_2}}{2(1 - C_p^2)} \quad (9)$$

$$C_m = -\frac{(C_1 + C_2) + \sqrt{(C_1 + C_2)^2 - 4C_1C_2(1 - C_p^{-2})}}{2} \quad (10)$$

where

$$C_p = \frac{1}{\sqrt{Q_1Q_2}}$$

and Q_1 and Q_2 are quality factors of the two resonant circuits.

Now using Equation (7) one can calculate the various antenna parameters for the proposed antenna, such as reflection coefficient, VSWR and return loss.

The reflection coefficient of the patch can be calculated as —

$$\Gamma = \frac{Z_0 - Z_T}{Z_0 + Z_T} \quad (11)$$

where Z_0 = characteristic impedance of the coaxial feed (50 ohm)

$$\text{VSWR} = \frac{1 + |\Gamma|}{1 - |\Gamma|} \quad (12)$$

and

$$\text{Return loss} = 20 \log |\Gamma| \quad (13)$$

3. RADIATION PATTERN

The radiation pattern for half U-slot loaded semicircular disk patch antenna is calculated as [22]

$$E(\theta) = J^n k_0 R V_0 e^{jk_0 r_1} [J_{n+1}(k_0 R \sin\theta) - J_{n-1}(k_0 R \sin\theta)] \cdot \cos n\phi \quad (14)$$

$$E(\phi) = J^n k_0 R V_0 e^{-jk_0 r_1} [J_{n+1}(k_0 R \sin\theta) - J_{n-1}(k_0 R \sin\theta)] \cdot \cos\theta \sin n\phi \quad (15)$$

where

V_0 = radiating edge voltage = $h_1 E_0 J_n(R)$
r_1 = distance of an arbitrary far-field point
R = radius of half circular fed disk patch

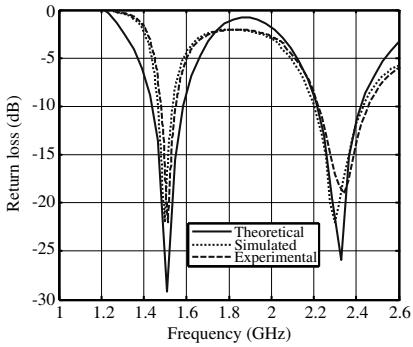

Figure 6. Comparative plot of return loss with frequency along with theoretical, simulated and experimental results (L_S = 46.2 mm, W_S = 6 mm, L_n = 6.0 mm, W_n = 2.5 mm, r = 1.0 mm, x_0 = 12.4 mm, h = 15 mm, $\varepsilon_r = 1.0$).

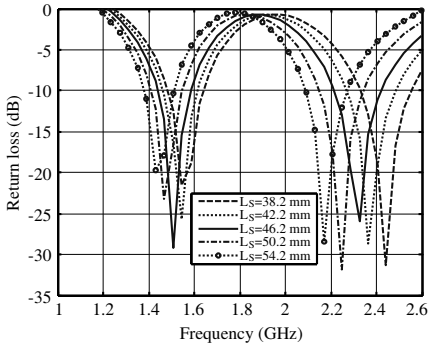

Figure 7. Variation of returns loss with frequency for different value of slot length 'L_S'.

4. DESIGN SPECIFICATIONS

Table 1. Design specification for half U-slot loaded half disk patch antenna.

Substrate material	air
Relative permittivity of the substrate (ε_r)	1.0
Thickness of the dielectric substrate (h)	15.0 mm
Radius of the half disk patch (R)	40.0 mm
Length of the slot (L_S)	46.2 mm
Width of the slot (W_S)	6.0 mm
Length of the notch (L_n)	6.0 mm
Depth of the notch (W_n)	2.5 mm
Feed location (x_0, y_0)	(12.6 mm, 0.0)

5. RESULTS AND DISCUSSION

The comparative plot of variation of return loss with frequency for half U-slot loaded semicircular disk patch antenna is shown in Fig. 6 along

with experimental [23] and simulated results using IE3D [24].

From the figure, It is observed that the antenna resonates at two frequencies ($fr_1 = 1.50\,\text{GHz}$, $fr_2 = 2.32\,\text{GHz}$, simulated $fr_1 = 1.49\,\text{GHz}$, $fr_2 = 2.29\,\text{GHz}$) and $-10\,\text{dB}$ bandwidth is found to be 5.96% for lower resonance whereas it is 11.08% for higher resonance frequency (simulated 5.03% and 11.15%). Frequency ratio of upper to lower resonance frequency is found to be 1.54 (simulated 1.53). The theoretical results are in good agreement with simulated and experimental results. It may be mentioned that both theoretical and simulated results for bandwidth are in good agreement at upper resonance frequency with experimental results whereas there is slight deviation at lower resonance frequency.

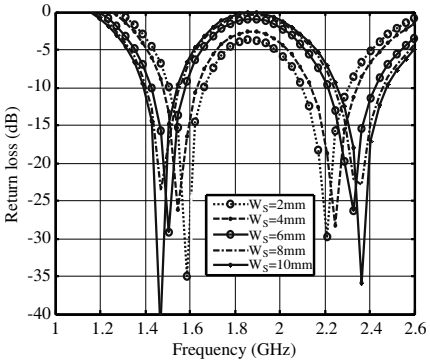

Figure 8. Variation of return loss with frequency for different value of slot width 'W_S'.

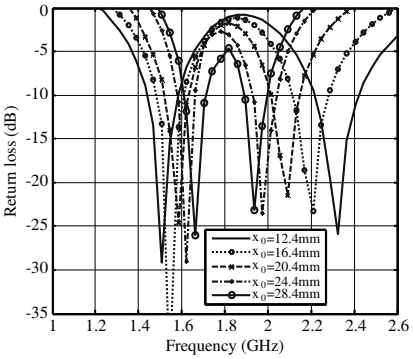

Figure 9. Variation of return loss with frequency for different value of feed point 'x_0'.

Table 2. Calculated bandwidth for different value of slot length.

Slot length	Lower resonance frequency			Upper resonance frequency		
(L_S)	Band-width (MHz)	Centre frequency (GHz)	Band-width (%)	Band-width (MHz)	Centre frequency (GHz)	Band-width (%)
38.2 mm	105	1.55	6.77%	278	2.44	11.39%
42.2 mm	97	1.54	6.30%	268	2.36	11.36%
46.2 mm	90	1.50	5.96%	257	2.32	11.08%
50.2 mm	78	1.46	5.34%	246	2.24	10.98%
54.2 mm	65	1.43	4.58%	232	2.17	10.69%

Figures 7 and 8 show the variation of return loss with frequency for the different value of slot length and slot width. From Fig. 7, it is found that lower and upper resonance frequency shifts towards lower side as the slot length increases and the bandwidth at both frequencies decreases as shown in Table 2, while for increasing the slot width slight variation in upper and lower resonance frequency is observed i.e., higher resonance frequency shifts to higher side and lower resonance frequency shifts to lower side and the bandwidth for different slot width are shown in Table 3. It is found that at lower resonance frequency the bandwidth depends inversely on the slot width whereas at upper resonance frequency the bandwidth depends directly on the slot width.

The variation of return loss with frequency with feed point and

Table 3. Calculated bandwidth for different value of slot width.

Slot width	Lower resonance frequency			Upper resonance frequency		
(W_S)	Band-width (MHz)	Centre frequency (GHz)	Band-width (%)	Band-width (MHz)	Centre frequency (GHz)	Band-width (%)
2.0 mm	99	1.58	6.27%	242	2.21	10.95%
4.0 mm	95	1.54	6.17%	249	2.26	11.02%
6.0 mm	90	1.50	5.96%	257	2.32	11.08%
8.0 mm	84	1.47	5.71%	262	2.34	11.20%
10.0 mm	81	1.45	5.59%	266	2.34	11.37%

Table 4. Calculated bandwidth for different value of probe feed point.

Feed point	Lower resonance frequency			Upper resonance frequency		
(x_0)	Band-width (MHz)	Centre frequency (GHz)	Band-width (%)	Band-width (MHz)	Centre frequency (GHz)	Band-width (%)
12.4 mm	90	1.50	5.96%	257	2.32	11.08%
16.4 mm	85	1.54	5.51%	230	2.20	10.45%
20.4 mm	77	1.58	4.90%	187	2.09	9.49%
24.4 mm	68	1.61	4.22%	177	1.97	8.90%
28.4 mm	60	1.64	3.66%	157	1.93	8.13%

probe radius is shown in Fig. 9 and Fig. 10. It is observed that for increasing the value of feed position, higher resonance frequency shifts towards the lower side whereas the lower resonance shifts slightly to higher side and bandwidth at both the resonances decreases as shown in Table 4, while with increasing probe radius both the resonance frequencies are shifted to higher resonance side and the bandwidth for different probe radii are shown in Table 5. It is observed from the table that bandwidth both at lower and upper resonance frequency depends directly on probe radius.

Figures 11 and 12 show the variation of frequency with slot length and slot width and it is observed that both lower and upper resonance frequency decreases for (1.55 GHz to 1.43 GHz and 2.44 GHz

Table 5. Calculated bandwidth for different value of probe radius.

probe radius	Lower resonance frequency			Upper resonance frequency		
(r)	Band-width (MHz)	Centre frequency (GHz)	Band-width (%)	Band-width (MHz)	Centre frequency (GHz)	Band-width (%)
0.6 mm	81	1.46	5.51%	232	2.21	10.50%
0.8 mm	85	1.47	5.78%	246	2.24	10.98%
1.0 mm	90	1.50	5.96%	257	2.32	11.08%
1.2 mm	98	1.54	6.36%	278	2.36	11.74%
1.4 mm	110	1.55	7.10%	287	2.44	11.76%

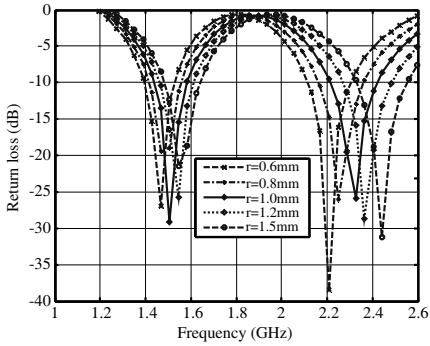

Figure 10. Variation of return loss with frequency for different value of probe radius 'r'.

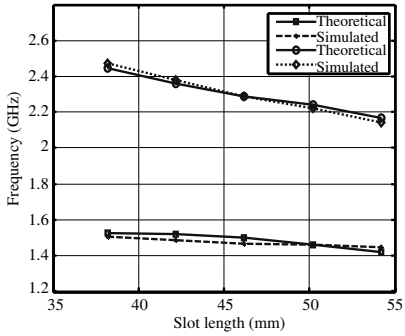

Figure 11. Variation of lower and upper resonance frequency for different value of slot length.

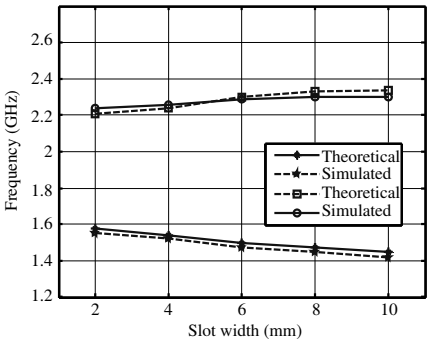

Figure 12. Variation of lower and upper resonance frequency for different value of slot width.

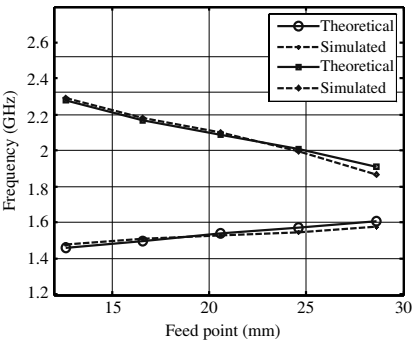

Figure 13. Variation of lower and upper resonance frequency for different value of feed point.

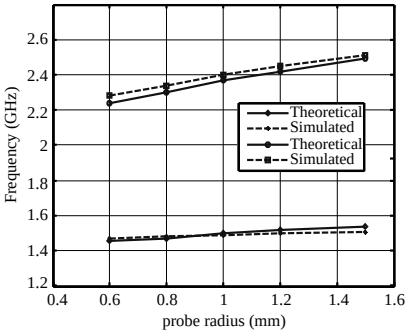

Figure 14. Variation of lower and upper resonance frequency for different value of probe radius.

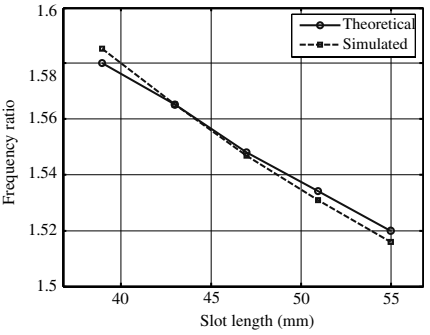

Figure 15. Variation of frequency ratio for different value of slot length.

to 2.17 GHz) for different value of slot length while the upper resonance frequency increases (2.21 GHz to 2.34 GHz) and lower resonance frequency decreases (1.58 GHz to 1.45 GHz) with increasing the slot width.

Figures 13 and 14 show the variation of frequency with different values of feed position and probe radius and it is observed that the upper resonance frequency decreases (2.32 GHz to 1.93 GHz) and the lower resonance frequency (1.50 GHz to 1.64 GHz) slightly increases with increasing the value of feed position, while the value of upper and lower resonance frequency both increases (2.21 GHz to 2.44 GHz and 1.46 GHz to 1.55 GHz) with increasing the probe radius.

Figures 15 and 16 show the ratio of resonance frequencies f_2/f_1

for different value of slot length and slot width. It is observed that the ratio of frequency decreases with increasing the value of slot length, while it increases with increasing the slot width.

Figures 17 and 18 show the ratio of resonance frequencies f_2/f_1 for different value of feed point and probe radius. It is found that the resonance frequency decreases with increasing the feed position, while it increases with increasing the probe radius.

From Fig. 19, it is found that the radiation pattern of the proposed antenna shows close agreement with the simulated results at both the resonance frequencies except in the off-beam directions and the directivity at higher resonance frequency is less as compared to lower resonance frequency.

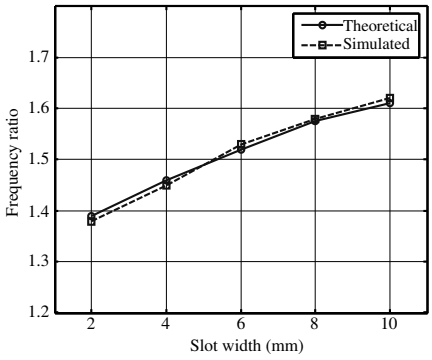

Figure 16. Variation of frequency ratio for different value of slot width.

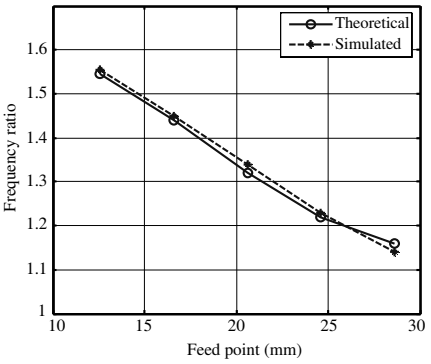

Figure 17. Variation of frequency ratio for different value of feed point.

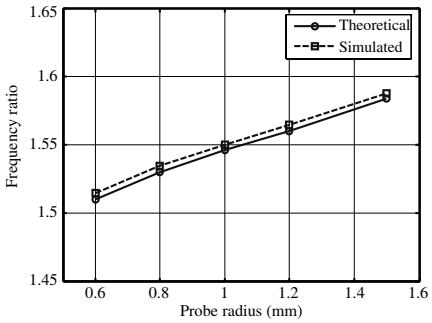

Figure 18. Variation of frequency ratio with different value of probe radius.

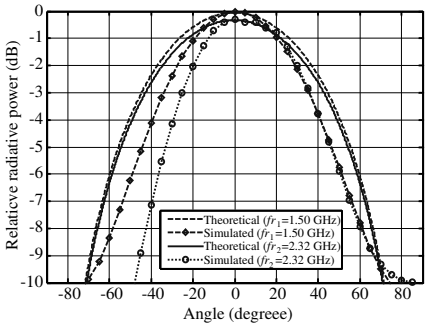

Figure 19. Radiation pattern for lower and upper resonance frequency of half U-slot loaded semicircular disk patch antenna.

6. CONCLUSION

From the analysis it is concluded that compact half U-slot loaded semicircular disk patch antenna can operate at two resonance frequencies 1.50/2.32 GHz and useful for various applications. The resonance frequency is highly dependent on the slot dimensions as well as probe radius and feed locations.

REFERENCES

1. Krishna, D. D., M. Gopikrishna, C. K. Aanandan, P. Mohanan, and K. Vasudevan, "Compact dualband slot loaded circular microstrip antenna with a superstrate," *Progress In Electromagnetic Research*, Vol. 83, 245–255, 2008.
2. Eldek, A., A. Z. Elsherbeni, and C. E. Smith, "Square slot antenna for the dual and wideband wireless communications systems," *Journal of Electromagnetic Waves and Applications*, Vol. 19, No. 12, 1571–1581, 2005.
3. Mishra, A., P. Singh, N. P. Yadav, J. A. Ansari, and B. R. Vishvakarama, "Compact shorted microstrip patch antenna for dualband operation," *Progress In Electromagnetic Research C*, Vol. 9, 171–192, 2009.
4. Singh, A. K. and M. K. Meshram, "Shorting pin loaded dualband compact rectangular microstrip patch antenna," *Int. Journal of Electronics*, Vol. 94,237–250, 2007.
5. Davison, S. E, S. A. Long, and W. F. Richards, "Dualband microstrip antenna with monolithic reactive loading," *Electron. Lett.*, Vol. 21, 936–937, 1985.
6. Daniel, A. E. and G. Kumar, "Tunable dual and triple frequency stub-loaded rectangular microstrip antennas," *IEEE Antennas and Propagation Society International Symposium*, 2140–2143, Newport Beach, CA, 1995.
7. Ysai, S. N., H. H. Hsin, H. K. Dia, and K. T. Cheng, "Arcuate slot antenna assembly," U.S. Patent No. 6373443, 2002.
8. Snowdon, R. A., "Slot antenna arrangement for portable personal computers," U.S. Patent No. 5677698, 1997.
9. Axelrod, A., M. Kisliuk, and J. Maoz, "Broadband microstrip fed slot radiator," *Microwave Journal*, Vol. 81–84, 1989.
10. Akhavan, H. G. and D. M. Syahkal, "Study of coupled slots antennas fed by microstrip lines," *The 10th Internationa Confrences on Antennas and Propagation*, 1290–1292, 1999.
11. Wong, K. L. and W. H. Hsu, "Broadband trigular microstrip

antenna with U- shaped slot," *Electron Lett.*, Vol. 33, 2085–2087, 1997.

12. Luk, K. M., K. F. Lee, and W. L. Tam, "Circular U-slot patch with dielectric substrate," *Electron. Lett.*, Vol. 33, 1000–1002, 1997.
13. Lee, K. F., K. M. Luk, K. F. Tong, S. M. Shum, T. Huynh, and R. Q. Lee, "Experimental and simulation studies of coaxially fed U-slot rectangular patch antenna," *IEE Proc. Micro. Antennas Propag.*, Vol. 144, 354–358, 1997.
14. Chen, L. C., et al., "Resonant frequency of circular disk printed circuit antenna," *IEEE Trans. Antenna Propag.*, Vol. 25, 595–596, 1997.
15. Garg, R., P. Bhartia, I. Bahl, and A. Ittipiboon, *Microstrip Antenna Design Handbook*, Artech House, Boston, London, 2003.
16. Kumar, G. and K. P. Ray., *Broadband Microstrip Antennas*, 74–79, Artech House, Boston, London, 2003.
17. Wolf, E. A., *Antenna Analysis*, Artech House, Narwood, USA, 1998.
18. Shivnarayan and B. R. Vishvakarma, "Analysis of inclined slot loaded patch for dualband operation," *Microwave Opt. Technology Lett.*, Vol. 48, 2436–2441, 2006.
19. Zhang, X. X. and F. N. Yang, "Study of slit cut on microstrip antenna and its application," *Microwave Opt. Technology Lett.*, Vol. 18, 297–300, 1998.
20. Bahal, I. J., *Lumped Elements for RF and Microwave Circuit*, 456–459, Artech House, 2003.
21. Balanis, C. A., *Antenna Theory Analysis and Design*, 2nd edition, Wiley, New York, 1997.
22. Meshram, M. K. and B. R. Vishvakarma, "Gap-coupled microstrip array antenna for wideband operation," *Int. Journal of Electronics*, Vol. 88, 1161–1175, 2001.
23. Ray, K. P. and D. D. Krishna, "Compact dualband suspended semicircular microstrip antenna with half U-slot," *Microwave Opt. Technology Lett.*, Vol. 48, 2021–2024, 2006.
24. Zeland software, Inc., IE3D simulation software, version 14.05 Zeland software, CA, 2008.